

● *Original Contribution*

ULTRASOUND BACKSCATTER AND ATTENUATION IN HUMAN LIVER WITH DIFFUSE DISEASE

ZHENG FENG LU,[†] J. A. ZAGZEBSKI[‡] and F. T. LEE[‡]

[†]Department of Radiology, Columbia University, New York, NY, USA; and [‡]Departments of Medical Physics and Radiology, University of Wisconsin, Madison, WI, USA

(Received 11 December 1998; in final form 30 March 1999)

Abstract—Ultrasound backscatter and attenuation in the liver were measured in patients with diffuse liver disease and in 35 volunteers who had no history of liver ailments. Measurements were done using radiofrequency (RF) echo signals derived from a clinical scanner; a reference phantom was scanned to account for effects of gain, transmit-receive frequency response and transducer beam patterns on echo data. The mean backscatter coefficient at 3 MHz in livers of 7 patients with fatty infiltration was $6.8 \times 10^{-3} \text{ cm}^{-1} \text{ sr}^{-1}$ compared to a mean of $0.5 \times 10^{-3} \text{ cm}^{-1} \text{ sr}^{-1}$ in healthy patients. Mean attenuation at 3 MHz was 2.54 dB/cm in fatty livers compared to 1.66 dB/cm in healthy patients. A total of 7 patients with end-stage liver disease (cirrhosis) had attenuation values similar to those in the healthy group, and their mean liver backscatter was somewhat greater than the mean backscatter for healthy livers. Quantitating both backscatter and attenuation should be considered for detecting fatty infiltration; additional processing methods are needed to differentiate cirrhotic changes on the basis of acoustic signals. © 1999 World Federation for Ultrasound in Medicine & Biology.

Key Words: Ultrasound, Attenuation coefficient, Backscatter coefficient, Phantoms, Liver, Diffuse liver disease, Fatty liver, Cirrhosis.

INTRODUCTION

Methods for detecting diffuse liver disease by ultrasound (US) have been a frequent topic of investigation in recent years. Many diffuse conditions, such as fatty infiltration of the liver, are accompanied by changes in ultrasound attenuation or backscatter relative to that of healthy liver. In severe cases, these changes are easily identified on grey-scale B-mode images of the liver because image brightness and the ability to penetrate are altered (Joseph et al. 1991; Withers and Wilson 1998). However, qualitative judgments of attenuation and echogenicity are not always reliable indicators of liver pathology (Castro et al. 1996; Hultcrantz and Gabrielsson 1993; Ochs et al. 1994; Garra 1993; Davies et al. 1991). One reason for this may be the lack of standardization and calibration of US imaging systems. This has prompted investigators to apply nonimaging, quantitative US methods to attempt to better characterize liver diseases (Maklad et al. 1984; Afschrift et al. 1987; Garra et al. 1987, 1989; Cloostermans et al. 1986; Parker et al. 1988; Hartman et al. 1991;

Layer et al. 1991; Garra 1993; Oosterveld et al. 1993; Lu et al. 1997).

The majority of ultrasound measurement techniques that have been applied to *in vivo* characterization of normal and abnormal human liver are restricted to attenuation properties of this organ. Unanimous agreement has been reached that the ultrasonic attenuation coefficient increases as the amount of pathologic fat in the liver increases (Wilson et al. 1984; Lin et al. 1988; Cloostermans et al. 1986; Kuni et al. 1989; Taylor et al. 1986). However, disagreement persists regarding the role played by fibrosis. In addition to attenuation, speed of sound (Chen et al. 1987; Lin et al. 1987) and scatterer spacing (Insana et al. 1986) have been investigated for detecting liver disease.

Contrary to the extensive volume of literature on attenuation, only a few reports have appeared quantifying backscatter levels from *in vivo* liver. The quantity used for measuring scattering from biological tissue is the backscatter coefficient (BSC), defined as the differential scattering cross-section per unit volume in the 180° direction (Sigelmann and Reid 1973). Because the BSC is related to “brightness” on grey-scale images, this parameter may be sensitive to subtle pathological changes

Address correspondence to: Dr. Zheng Feng Lu, Dept of Radiology, Columbia University, Milstein 2-128, 177 Fort Washington Ave, New York, NY 10032 USA. E-mail: zfl1@columbia.edu

in tissue. *In vivo* backscatter levels measured for healthy liver (O'Donnell and Reilly 1985; Boote et al. 1992; Zagzebski et al. 1993) are in fair agreement with earlier published *in vitro* results (Bamber and Hill 1981; Nicholas 1982). Cirrhotic livers were found to exhibit elevated backscatter levels in one study (O'Donnell and Reilly 1985). Steroid hepatopathy is accompanied by noticeable elevations in the backscatter coefficient (O'Brien et al. 1996; Lu et al. 1997). Osawa and Mori (1996) found grey-level histograms useful for differentiating healthy from fatty liver using B-mode images, but these provide relative backscatter levels only.

The work described in this paper resulted in initial data on the US backscatter coefficient in patients with diffuse liver disease for comparison with values of this parameter in livers of healthy individuals. Both the attenuation coefficient and the backscatter coefficient were measured in livers of patients with no history of liver disease and of patients with diffuse disease. One group of patients was diagnosed with fatty infiltrated liver and a second group had cirrhosis. Quantitative backscatter images were computed from digitized RF echo data, and backscatter and attenuation levels were determined.

METHODS

Subjects

A total of 35 healthy individuals and 14 patients with diffuse liver disease were included in the study. The healthy volunteers ranged from 15 to 68 y old, with a mean age of 40 y. Each volunteer filled out a questionnaire containing queries related to the condition of his/her liver, such as the degree of alcoholic consumption (less than one drink a day allowed for participation) and if they recalled being exposed to specific hepatoxins (would disqualify the subject from the study).

Among the 14 patients, 7 had CT diagnosed fatty infiltration, indicated when Hounsfield units in noncontrast images of the liver were lower than those of the spleen (Gedgudas-McClees et al. 1994). The ultrasound scan was usually done on the same day as the CT scan. A total of 7 patients had end-stage liver disease with cirrhosis and were awaiting transplant surgery at University of Wisconsin Hospitals. The study was done under an approved institutional protocol, and subjects signed consent forms after the nature of the procedures had been fully explained.

Echo data acquisition

Figure 1 outlines the experimental apparatus used in this study. A Siemens scanner (Model SL-1, Siemens Medical System, Inc., Issaquah, WA) equipped with mechanical sector transducers was used to acquire echo data. This scanner has been modified by the

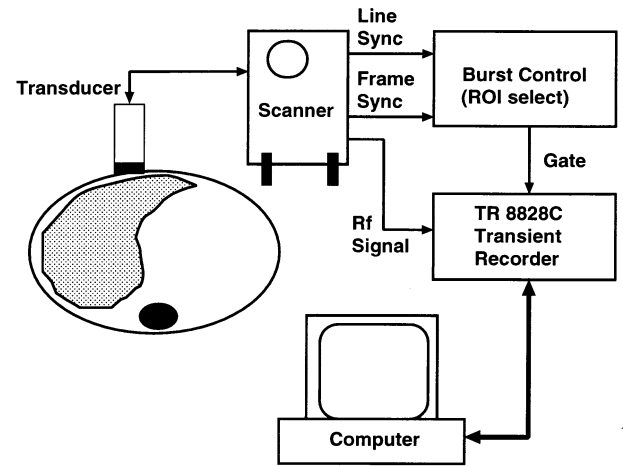


Fig. 1. Data-acquisition system for acquiring radiofrequency echo data from the liver. A Siemens SL100 scanner equipped with mechanical transducers was used.

manufacturer to enable acquisition of unprocessed RF echo signals. These RF signals were digitized with 8-bit resolution at a sampling rate of 50 MHz by a LeCroy TR8828C transient recorder equipped with a 768 kb buffer memory. The data were then transferred to a Vax-station via a GPIB interface and stored on disk. Line and frame synchronization pulses from the scanner were applied to a burst control circuit to enable selection of specific beam lines in the image sector, thus limiting the data acquisition to a well-defined region-of-interest (ROI).

Four scans of the right lobe of the liver were made in closely spaced, parallel planes with hand-held probes. Data were acquired using a 3.5-MHz and a 5-MHz transducer, with the probe positioned just below the rib cage. Each scanning plane provided RF data from 90 acoustic lines, each separated by approximately 1° . The recorded signal began 2.3 cm beneath the surface of the body wall and extended to a depth of 12 cm.

RF echo signals from a "reference phantom" were also acquired using the same transducer, region-of-interest selection and scanner settings. When acquiring reference data, the transducer was placed in direct contact with the tissue-mimicking (TM) material of the phantom (Fig. 2). The attenuation and backscatter coefficients for the TM material had been measured using standard laboratory methods (Madsen et al. 1982; Chen et al. 1993) applied to cylindrical test samples of the reference phantom material. The phantom contains water-based gel with n-propyl alcohol added to produce a tissue-like speed of sound, 1538 m/s (Burlew et al. 1980). Graphite powder mixed into the gel provides an attenuation coefficient of $0.48 f + 0.016 f^2$ dB/cm, where f is the ultrasound frequency in MHz. This value is close to the

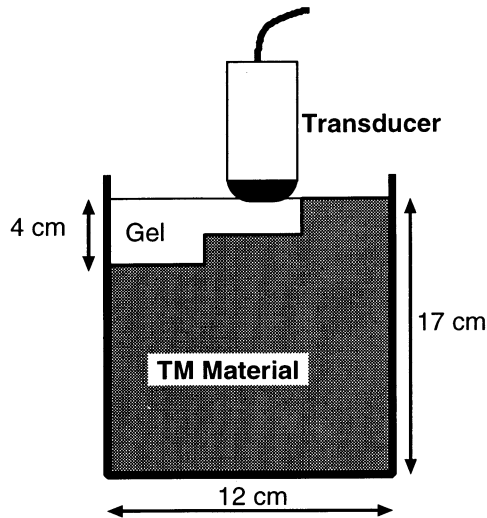


Fig. 2. Schematic of the reference phantom for the clinical liver study. When recording data, the transducer was placed in direct contact with the tissue-mimicking (TM) material, or in contact with a low attenuating gel when reference data were acquired for scans of patients with ascites.

attenuation coefficient of healthy liver tissue. Microscopic glass beads, with an average diameter of $60.5 \mu\text{m}$, were mixed into the gel to provide a scattering level similar to that of healthy liver tissue for the analysis frequency range.

In most patients with cirrhosis, ascites was also present. The extent of ascites varied, but the beam path through fluid could be as much as 5 cm. To make the echo level from the reference phantom as close as possible to the echo level obtained from the liver, without the need to change receiver sensitivity settings in the scanner, two low attenuating offsets that represented the low acoustic attenuation in ascites fluid were available in the phantom (Fig. 2). An offset thickness of 2 cm or 4 cm could be chosen for the reference signals, depending on the degree of ascites in the patient. The offset consists of gel with an attenuation of 0.06 dB/cm/MHz .

After RF data acquisition, subjects were scanned with a 7.5-MHz transducer to image the superficial tissue region in the vicinity of the scanned volume. The transducer orientation was the same as that used in the data-acquisition phase, and an attempt was made to apply the same pressure on the body wall as was used in the RF echo data acquisition. Because the tip of the 7.5-MHz probe was of the same geometry as the 3.5-MHz and 5-MHz transducers, it was assumed that the body wall was distorted to the same degree in both scans. A small field-of-view, high-magnification image was recorded with the 7.5-MHz probe. This was then used to estimate the amount of body wall fat and muscle in the scanning plane.

Signal analysis

Data were analyzed using methods similar to those described previously (Lu *et al.* 1997; Zagzebski *et al.* 1993). First, signals along each beam line were branched into two channels, multiplying signals in one channel by $\sin \omega_o t$, and in the other by $\cos \omega_o t$, where ω_o is the analysis frequency and t is the echo arrival time. Analysis frequencies ranging from 2.25 MHz to 3.75 MHz were used for the 3.5-MHz transducer signals, and frequencies from 4.0 MHz to 5.5 MHz were used for data obtained with the 5-MHz probe. Signals were then convolved with a sliding, $4\text{-}\mu\text{s}$ Blackman Harris window, which served as a low-pass filter. The intervals between centers of the $4\text{-}\mu\text{s}$ overlapping data segments were $0.64 \mu\text{s}$, corresponding to an axial distance of 0.5 mm. Filtered echo signals in each quadrature channel were squared and added for each 0.5-mm signal segment in each beam line.

The same analysis was applied to the echo signal data from the reference phantom. We then computed $ri(\omega_o, l, z)$, the ratio of the echo signal intensity at frequency ω_o from depth z along beam line l within a liver ROI, to the mean signal intensity from depth z in the reference phantom. The mean is over beam lines and scan planes for the echo data from the reference. Our analysis shows that this ratio is independent of the ultrasound instrument and transducer beam properties, and that it depends only on the acoustic properties of the sample and reference (Yao *et al.* 1990).

For a uniform region in the sample, the logarithm of $ri(\omega_o, l, z)$ vs. z forms a straight line. The slope of this line is proportional to the difference between the attenuation coefficient of the liver and that of the reference phantom. Because the latter is known, the attenuation in the sample can be deduced. Quantitative “backscatter estimator” images of an ROI in the liver are produced by compensating the intensity ratio data for attenuation along the acoustic path in the liver and any excess attenuation between the transducer and ROI (see next section), and multiplying by the backscatter coefficient of the reference phantom.

Overlying layer correction

The 7.5-MHz images of the body wall were used to estimate thicknesses of fat, muscle and ascites (if present) in the patient over the region scanned with the lower frequency transducers. Table 1 summarizes data on the thicknesses of the body wall components measured in this study. The overlying tissue includes layers of fat, muscle, ascites and liver tissue, and was represented by the model shown in Fig. 3. Here h_{fat} , h_{muscle} , h_{ascites} and h_{liver} are estimated thicknesses of the respective components. Correspondingly, the overlying path in the reference phantom includes the tissue-mimicking

Table 1. Thicknesses of body wall components measured in this study.

	Average	Maximum	Minimum
Thickness of fat layer (mm)	6.77	14.0	3.0
Thickness of muscle layer (mm)	8.4	16.0	2.5

background material, with thickness h_{ref} , and the low attenuating gelatin layer whose thickness is h_{gel} . $\Delta_{\text{O.L.}}$, the difference between the attenuation in the path overlying the liver ROI and that overlying the ROI in the reference phantom is estimated as follows:

$$\Delta_{\text{O.L.}} = (\alpha_{\text{fat}} f h_{\text{fat}} + \alpha_{\text{muscle}} f h_{\text{muscle}} + \alpha_{\text{ascites}} f h_{\text{ascites}} + \alpha_{\text{liver}} f h_{\text{liver}}) - (\alpha_{\text{gel}} f h_{\text{gel}} + \alpha_{\text{ref}}(f) h_{\text{ref}}) \quad (1)$$

where α_{fat} , α_{muscle} , and α_{ascites} are the attenuation coefficient slopes of fat, muscle and ascites fluid, respectively and f is the frequency in MHz. Values used were 0.6 dB/cm/MHz, 1.3 dB/cm/MHz and 0.1 dB/cm/MHz respectively for fat, muscle and ascites (Goss et al. 1978). α_{liver} is a measured quantity. α_{gel} is the attenuation coefficient of the ascites-mimicking gelatin in the reference phantom, 0.06 dB/cm/MHz. $\alpha_{\text{ref}}(f)$ is the attenuation coefficient of the tissue-mimicking background material in the reference phantom, $0.48f + 0.016f^2$ dB/cm. Note the attenuation and thickness of the ascites fluid is included for generality but, in most cases, h_{ascites} is zero. If the reference phantom was scanned without the low attenuating layer, h_{gel} is zero.

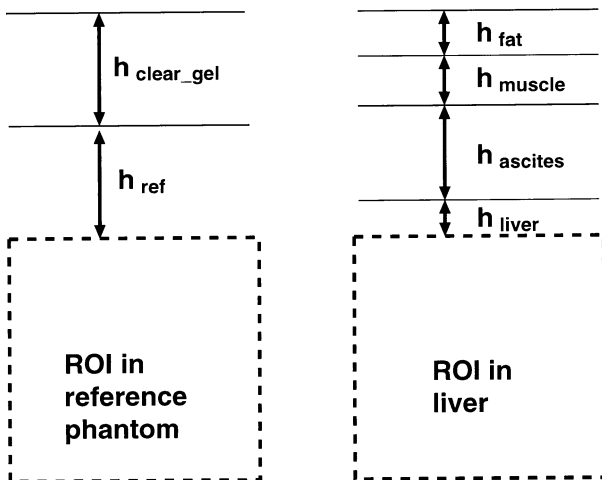


Fig. 3. Model used to correct backscatter estimators for presence of overlying tissue layers in subjects.

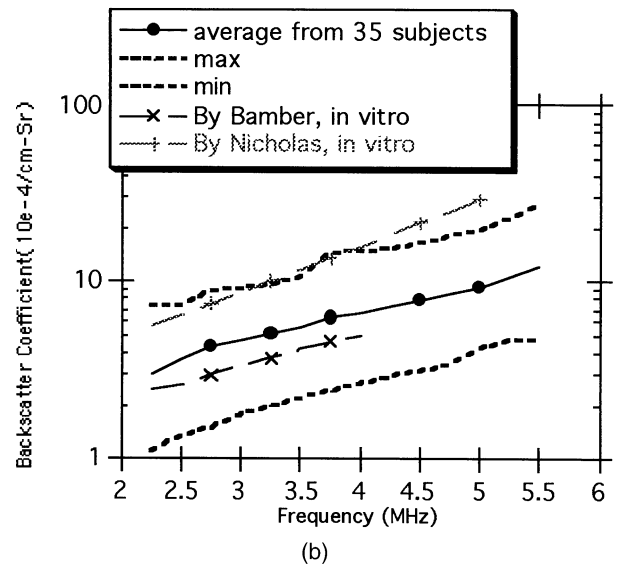
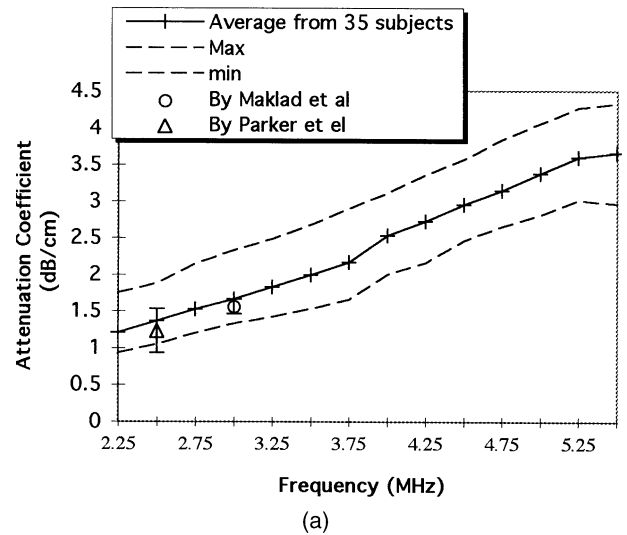


Fig. 4. (a) Attenuation coefficient vs. frequency in livers of 35 healthy volunteers. Also shown are results for healthy patients published by Maklad (\circ) and by Parker (\triangle). Maximum and minimum measured values are also indicated. (b) Backscatter coefficient vs. frequency for healthy subjects. Additional data points are shown for *in vitro* measurements by Bamber and Nicholas. Maximum and minimum measured values are also indicated.

RESULTS

Healthy livers

Figure 4a presents measured attenuation results for healthy patients. Among the 35 healthy subjects, the average attenuation coefficient in liver tissue at 3 MHz is 1.66 dB/cm, with a standard deviation of 0.21 dB/cm. These results agree very well with other researchers' *in vivo* estimates of the attenuation of healthy liver. Previously observed attenuation values were 0.52 ± 0.03

dB/cm/MHz at 3 MHz (Maklad *et al.* 1984) and $0.47 \text{ dB/cm/MHz} \times f^n$ where f is the frequency in MHz and $n = 1.05 \pm 0.25$ (Parker *et al.* 1988). These values are indicated on the graph.

Figure 4b presents the average and range of backscatter coefficients vs. frequency for all 35 healthy subjects. The average and standard deviation of the backscatter coefficient at 2.25 MHz for the healthy patients is $0.3 \pm 1.62 \times 10^{-3} \text{ cm}^{-1}\text{sr}^{-1}$, agreeing very well with previous *in vivo* results using a 2.25-MHz transducer, reported by O'Donnell and Reilly (1985). They found an average backscatter coefficient of $3.5 \times 10^{-4} \text{ cm}^{-1}\text{sr}^{-1}$ in 13 healthy subjects, though they used a different estimation for body wall losses, and analyzed envelope-detected echo signals from the scan converter of a clinical ultrasound imager, rather than RF echo signals as in our work. Also shown in Fig. 4b are backscatter coefficients measured on *in vitro* liver samples by Nicholas (1982) and by Bamber and Hill (1981). The measured backscatter coefficients in our study appear to be between those of these earlier workers.

Fatty infiltrated liver

The results measured from the group of patients with fatty livers are compared with the normal range in Fig. 5. The average attenuation coefficient at 3 MHz for fatty infiltrated liver patients is 2.54 dB/cm with a SD of 0.25 dB/cm (Fig. 5a). This compares with an average of 1.66 dB/cm at 3 MHz in healthy subjects. Though not surprising from clinical results, it is clear that fatty infiltration significantly elevates the attenuation of liver tissue. The average backscatter coefficient at 3 MHz for fatty infiltrated liver patients is $6.8 \times 10^{-3} \text{ cm}^{-1}\text{sr}^{-1}$ with an SD of $3.7 \times 10^{-3} \text{ cm}^{-1}\text{sr}^{-1}$ (Fig. 5b). This is about 14 times higher than the average result seen in the healthy group at 3 MHz, $0.5 \times 10^{-3} \text{ cm}^{-1}\text{sr}^{-1}$. All 7 fatty livers have higher scattering levels than the healthy range.

Cirrhotic liver

As shown in Fig. 6, attenuation and backscatter in the group of cirrhotic liver patients do not differ significantly from those of healthy subjects, at least over the US frequency range investigated. The average attenuation coefficient at 3 MHz for cirrhotic livers is 1.76 dB/cm with an SD of 0.31 dB/cm (Fig. 6a). This is only slightly higher than the average for healthy patients (1.66 dB/cm at 3 MHz). The average backscatter coefficient at 3 MHz for cirrhotic livers is $1.4 \times 10^{-3} \text{ cm}^{-1}\text{sr}^{-1}$ with an SD of $1.8 \times 10^{-3} \text{ cm}^{-1}\text{sr}^{-1}$ (Fig. 6b). Significant overlap exists among the ultrasonic parameters from the cirrhotic liver patients and those from healthy individuals.

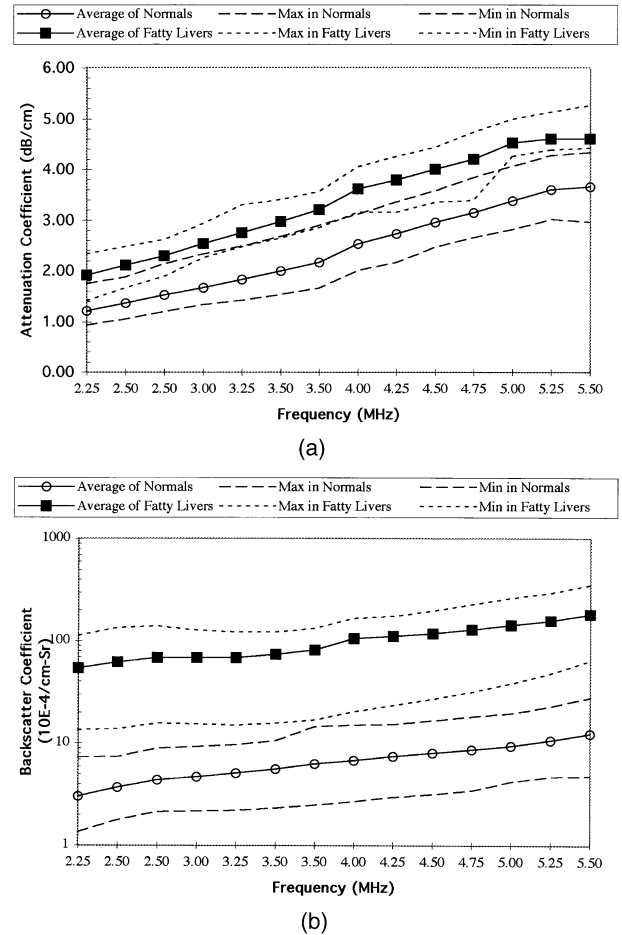


Fig. 5. Comparison of mean and range of attenuation and backscatter coefficients in fatty infiltrated livers and in healthy livers. (a) Attenuation coefficients vs. frequency. (b) Backscatter coefficients vs. frequency.

Differentiation among groups

In Fig. 7, two parameters, the attenuation coefficient slope and the average backscatter coefficient over the frequency range 2.25–3.75 MHz, are chosen as the two axes in a double-parameter display of data from the subject groups. The 35 healthy subjects are grouped to outline the “normal” range in the figure. Fatty livers, with higher attenuation and higher backscattering, are obviously separated from the “normal” range. The cirrhotic livers, with a wide variation of scatter and attenuation among subjects within this group, are poorly separated from healthy patients. Nevertheless, higher backscatter coefficients and slightly higher attenuation coefficients are observed in some of the cirrhotic livers.

DISCUSSION

Diffuse liver disease is a common clinical condition. The severity and extent of the disease ranges from

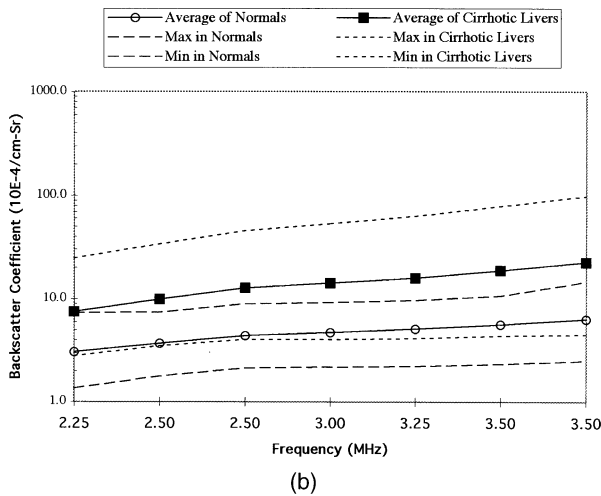
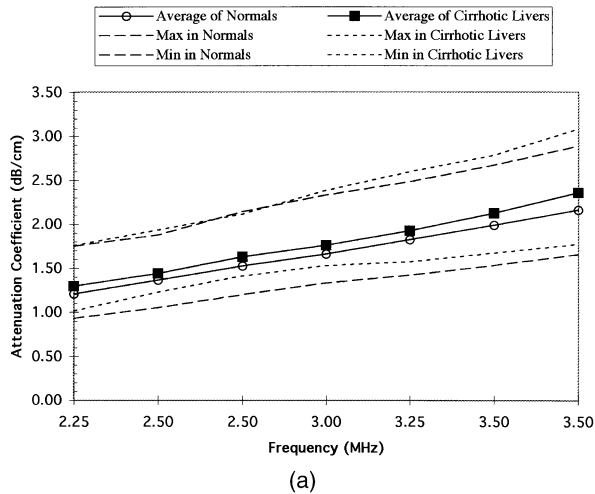


Fig. 6. Comparison of mean and range of attenuation and backscatter coefficients in cirrhotic livers and in healthy livers. (a) Attenuation coefficients vs. frequency. (b) Backscatter coefficients vs. frequency.

mild fatty infiltration to cirrhosis and end-stage liver disease. Although early fatty infiltration is usually presumed benign and reversible if proper treatment is carried out (Marn et al. 1991), evidence has been presented that some liver steatosis may progress to cirrhosis, especially if alcohol consumption is involved (Teli et al. 1995) or if inflammation is present (Powell et al. 1990). Because most cirrhosis and end-stage liver disease is irreversible and a liver transplantation is a final choice of therapy, detecting and monitoring the condition of fatty liver infiltration early in its course could provide better chances of cure or prolong the time of survival before irreversible change occurs. Also, in a rare but potentially fatal disease of acute fatty liver of pregnancy, early diagnosis may facilitate more aggressive management in

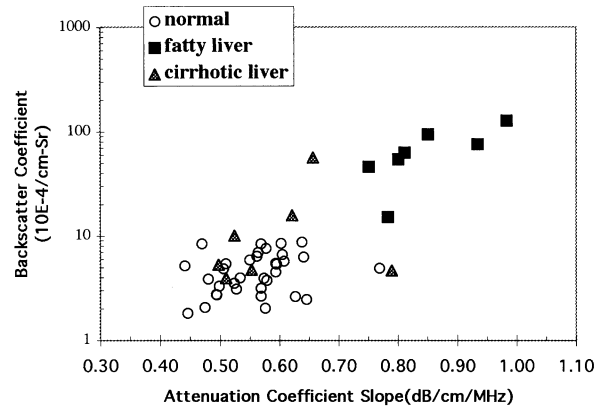


Fig. 7. Double-parameter display of the ultrasonic attenuation vs. the backscatter level in the liver of individual subjects. Shown are the attenuation coefficient slope and the average backscatter coefficient over the frequency range 2.25–3.75 MHz.

these patients, which could reduce mortality (Usta et al. 1994; Crockett et al. 1994; Castro et al. 1996).

In this paper, backscatter coefficients and attenuation coefficients were measured for livers of patients with diffuse liver disease and compared with values obtained from a group of individuals with no history of liver disease. Both the average attenuation coefficient and the backscatter coefficient in our measurements from healthy patients agreed with previous investigators' results. Comparison of data from 35 healthy subjects and 14 patients with diffuse liver disease shows that both the attenuation coefficient and the backscatter coefficient are elevated in fatty liver. The ultrasonic parameters exhibited strong discriminating power ($p < 0.001$) to differentiate between fatty liver and healthy patients in this group. This suggests a potential usefulness of the method for diagnosing the presence of fatty infiltration in the liver or monitoring effects on the liver during hepatotoxic drug treatment. Computed tomography (CT) has been used to identify moderate and severe fatty infiltration, but not mild fatty infiltration (Gedgaudas-McClees et al. 1994; Ricci et al. 1997). In addition, although conventional spin-echo (SE) MR images are insensitive for diagnosing fatty liver, recent research demonstrates improved results by comparing in-phase and opposed-phase MR images (Mitchell et al. 1991) or by using MRI spectroscopy (Ricci et al. 1997; Longo et al. 1993). However, CT and MRI are expensive, and a noninvasive means with US of quantitatively assessing fatty and fibrotic changes would be an advance in medical care. Because the fatty livers included in our study were detected by CT, the fatty infiltration was at moderate/severe stages. Future studies will be directed toward those patients with mild fatty infiltration, correlating the features

from US backscatter images with results from other studies.

It would be useful if quantitative methods provided greater differentiation between patients with cirrhosis and with healthy livers, but backscatter and attenuation in this frequency range was not effective. Our measurements suggest that elevation of the attenuation and backscatter coefficients in fatty liver is greater than that in cirrhotic liver. It is common that fibrotic livers exhibit varying degrees of fatty infiltration (Gedgudas-McClees *et al.* 1994), making the sonographic-pathologic correlation complicated due to different roles played by fibrosis and steatosis on the attenuation and backscatter coefficients (Garra 1993). Future investigations will include scatterer size and spacing measurements (Suzuki *et al.* 1993; Insana *et al.* 1986), including obtaining data over a broader frequency range to attempt to improve the diagnosis.

Acknowledgements—The authors are grateful to Dr. Ernest Madsen and Gary Frank for manufacturing the reference phantom. This work was supported in part by PHS Grant R01CA39224 from the National Institutes of Health.

REFERENCES

- Afschrift M, Cuvelier C, Ringoir S, Barbier F. Influence of pathological state on the acoustic attenuation coefficient slope of liver. *Ultrasound Med Biol* 1987;13:135–139.
- Bamber JC, Hill CR. Acoustic properties of normal and cancerous human liver - I. dependence on pathologic condition. *Ultrasound Med Biol* 1981;7:121–133.
- Boote EJ, Zagzebski JA, Madsen EL. Backscatter coefficient imaging using a clinical scanner. *Med Physics* 1992;19:1145–1152.
- Burlew MM, Madsen EL, Zagzebski JA, *et al.* A new ultrasound tissue-equivalent material. *Radiology* 1980;134:517–520.
- Castro MA, Ouzounian JG, Colletti PM, *et al.* Radiologic studies in acute fatty liver of pregnancy—a review of the literature and 19 new cases. *J Reproductive Med* 1996;41:839–843.
- Chen CF, Robinson DE, Wilson LS, *et al.* Clinical sound speed measurement in liver and spleen *in vivo*. *Ultrasonic Imaging* 1987;9:221–235.
- Chen J, Zagzebski J, Madsen E. Evaluation of a broad bandwidth method for measuring backscatter coefficients. *IEEE Trans Ultrason Ferro Freq Cont* 1993;40:603–607.
- Cloostermans MJTM, Mol H, Verhoef WA, Thijssen JM. *In vitro* estimation of acoustic parameters of the liver and correlations with histology. *Ultrasound Med Biol* 1986;12:39–51.
- Crockett HC, de Virgilio C, Shimaoka E, *et al.* Acute fatty liver of pregnancy: laparoscopy-assisted diagnosis. *Surg Laparosc Endosc* 1994;4:230–233.
- Davies RJ, Saverymuttu SH, Fallowfield M, Joseph AE. Paradoxical lack of ultrasound attenuation with gross fatty change in liver. *Clin Radiol* 1991;43:393–396.
- Garra BS. *In vivo* liver and splenic tissue characterization by scattering. In: Shung KK, Thieme GA, eds. *Ultrasonic scattering in biological tissues*. Boca Raton, FL: CRC Press, 1993:371–374.
- Garra BS, Insana MF, Shawker TH, Russell MA. Quantitative estimation of liver attenuation and echogenicity: normal state versus diffuse liver disease. *Radiology* 1987;162:61–67.
- Garra BS, Insana MF, Shawker TH, *et al.* Quantitative ultrasonic detection and classification of diffuse liver disease; comparison with human performance. *Invest Radiol* 1989;24:196–203.
- Gedgudas-McClees RK, Bernardino ME, Phillips VM. The liver and spleen. In: Putman CE, Ravin CE, eds. *Textbook of diagnostic imaging*. 2nd ed. Philadelphia: W.B. Saunders Co, 1994:887–890.
- Goss SA, Johnston RL, Dunn F. Comprehensive compilation of empirical ultrasonic properties of mammalian tissues. *J Acoust Soc Am* 1978;64:423–457.
- Hartman PC, Oosterveld BJ, Thijssen JM, Rosenbusch GJE. Variability of quantitative echographic parameters of the liver: intra- and interindividual spread, temporal- and age-related effects. *Ultrasound Med Biol* 1991;17:857–867.
- Hultcrantz R, Gabrielsson N. Patients with persistent elevation of aminotransferases: investigation with ultrasonography, radionuclide imaging and liver biopsy. *J Int Med* 1993;233:7–12.
- Insana MF, Wagner RF, Garra BS, *et al.* Pattern recognition methods for optimizing multivariate signatures in diagnostic ultrasound. *Ultrason Imaging* 1986;8:165–180.
- Joseph AE, Saverymuttu SH, al-Sam S, *et al.* Comparison of liver histology with ultrasonography in assessing diffuse parenchymal liver disease. *Clin Radiol* 1991;43:26–31.
- Kuni CC, Johnson TK, Crass JR, Snover DC. Correlation of Fourier spectral shift-determined hepatic acoustic attenuation coefficients with liver biopsy findings. *J Ultrasound Med* 1989;8:631–634.
- Layer G, Zuna I, Lorenz A, *et al.* Computerized ultrasound B-scan texture analysis of experimental diffuse parenchymal liver disease: correlation with histopathology and tissue composition. *J Clin Ultrasound* 1991;19:193–201.
- Lin T, Ophir J, Potter G. Correlation of sound speed with tissue constituents in normal and diffuse liver disease. *Ultrason Imaging* 1987;9:29–40.
- Lin T, Ophir J, Potter G. Correlation of ultrasonic attenuation with pathologic fat and fibrosis in liver disease. *Ultrasound Med Biol* 1988;14:729–734.
- Longo R, Ricci C, Masutti F, *et al.* Fatty infiltration of the liver. Quantification by 1H localized magnetic resonance spectroscopy and comparisons with computed tomography. *Invest Radiol* 1993;28:297–302.
- Lu ZF, Zagzebski JA, O'Brien RT, Steinberg H. Ultrasound attenuation and backscatter in the liver during prednisone administration. *Ultrasound Med Biol* 1997;23:1–8.
- Madsen EL, Zagzebski JA, Frank G. Oil-in-gelatin dispersions for use as ultrasonically tissue-mimicking materials. *Ultrasound Med Biol* 1982;8:277–287.
- Maklad N, Ophir J, Balsera V. Attenuation of ultrasound in normal liver and diffuse liver disease *in vivo*. *Ultrason Imaging* 1984;6:117–125.
- Marn CS, Bree RL, Silver TM. Ultrasonography of liver: technique and focal and diffuse liver disease. *Radiol Clin North Am* 1991;29:1151–1170.
- Mitchell DG, Kim I, Chang TS, *et al.* Fatty liver: chemical shift saturation and phase-difference MR imaging techniques in animals, phantoms and humans. *Invest Radiol* 1991;26:1041–1052.
- Nicholas D. Analysis of backscattering coefficients for excised human tissues: results, interpretation and associated measurements. *Ultrasound Med Biol* 1982;8:17–28.
- O'Brien RT, Zagzebski JA, Lu ZF, Steinberg H. Measurement of acoustic backscatter and attenuation in the liver of dogs with experimentally induced steroid hepatopathy. *Am J Vet Res* 1996;57:1690–1694.
- Ochs A, Rottler RM, Scholmerich J. Clinical relevance of abnormal liver findings with ultrasound. *Hepato-Gastroenterol* 1994;41:9–15.
- O'Donnell M, Reilly HF. Clinical evaluation of the B' scan. *IEEE Trans Sonics Ultrason* 1985;SU-32:450–457.
- Oosterveld BJ, Thijssen JM, Hartman PC, Rosenbusch GJE. Detection of diffuse liver disease by quantitative echography: dependence on *a priori* choice of parameters. *Ultrasound Med Biol* 1993;19:21–25.
- Osawa H, Mori Y. Sonographic diagnosis of fatty liver using a histogram technique that compares liver and renal cortical echo amplitudes. *J Clin Ultrasound* 1996;24:25–29.
- Parker KJ, Asztely MS, Lerner RM, *et al.* *In vivo* measurements of ultrasound attenuation in normal or diseased liver. *Ultrasound Med Biol* 1988;14:127–136.
- Powell EE, Cooksley WG, Hanson R, *et al.* The natural history of nonalcoholic steatohepatitis: A follow-up study of forty-two patients for up to 21 years. *Hepatology* 1990;11:74–80.

- Ricci C, Longo R, Gioulis E, et al. Noninvasive *in vivo* quantitative assessment of fat content in human liver. *J Hepatol* 1997;27:108–113.
- Sigelmann RA, Reid JM. Analysis and measurement of ultrasound from an ensemble of scatterers excited by sine-wave bursts. *J Acoust Soc Am* 1973;53:1351–1355.
- Suzuki K, Hayashi N, Sasaki Y, et al. Evaluation of structural changes in diffuse liver disease with frequency domain analysis of ultrasound. *Hepatology* 1993;17:1041–1046.
- Taylor KJW, Riely CA, Hammers L, et al. Quantitative US attenuation in normal liver and in patients with diffuse liver disease: importance of fat. *Radiology* 1986;160:65–71.
- Teli MR, Day CP, Burt AD, et al. Determinants of progression to cirrhosis or fibrosis in pure alcoholic fatty liver. *Lancet* 1995;346:987–990.
- Usta IM, Barton JR, Amon EA, et al. Acute fatty liver of pregnancy: An experience in the diagnosis and management of fourteen cases. *Am J Obstet Gynecol* 1994;171:1342–1347.
- Wilson L, Robinson D, Doust B. Frequency domain processing for ultrasonic attenuation measurement in liver. *Ultrason Imaging* 1984;6:278–292.
- Withers CE, Wilson SR. The liver. In: Rumack C, Wilson S, Charboneau JW, eds. *Diagnostic ultrasound*. St Louis, MO: Mosby, 1998: 110–114.
- Yao L, Zagzebski JA, Madsen EL. Backscatter coefficient measurements using a reference phantom to extract depth-dependent instrumentation factors. *Ultrason Imaging* 1990;12:58–70.
- Zagzebski JA, Lu Z, Yao L. Quantitative ultrasound imaging: *in vivo* results in normal liver. *Ultrason Imaging* 1993;15:335–351.